THEORY AND TECHNOLOGY OF PARTICLE ACCELERATION

https://doi.org/10.46813/2021-136-046

RARE-EARTH PERMANENT MAGNETS AND THEIR APPLICATION IN MAGNETIC SYSTEMS OF TECHNOLOGICAL ELECTRON ACCELERATORS

V.A. Bovda, A.M. Bovda, I.S. Guk, V.N. Lyashchenko, A.O. Mytsykov, L.V. Onischenko
National Science Center "Kharkov Institute of Physics and Technology", Kharkiv, Ukraine
E-mail: guk@kipt.kharkov.ua

High performance rare-earth permanent magnets become crucial components of modern electron accelerators. PLP (pressless process) method was described as the advanced production step in the current rare-earth permanent magnet manufacturing. The radiation resistance of SmCo and Nd-Fe-B magnets under electron beam with 10 and 23 MeV and bremsstrahlung were studied. Dipole magnetic systems on the base of rare-earth permanent magnets were designed for the technological electron accelerators at NSC KIPT.

PACS: 85.70.Sq; 75.50.Ww

INTRODUCTION

Permanent magnets have become a key component of electron beam transport lines mostly due to economic reasons.

Permanent magnets are mainly used on accelerators operating at constant beam energy or in a narrow energy range not requiring readjustment of the beam transport paths. The use of permanent magnets leads to significant savings in electricity and less expensive supplementary production. Permanent magnets do not require complex power supply systems and do not consume electricity for their operation [1 - 3].

Literature review and our works have shown that there is no universal design of a magnetic system for electron accelerators. They perform complex tasks and their magnetic systems require ad hoc optimization in each case.

The widespread use of permanent magnets in acceleration technologies began with advances in the development of materials based on Sm_2Co_{17} and $Nd_2Fe_{14}B$ alloys.

1. THE ORIGIN OF THE HIGH MAGNETIC PERFORMANCE OF RARE-EARTH PERMANENT MAGNETS

There is considerable interest in high performance Nd-Fe-B permanent magnets for use in charge particles accelerators [1]. The right choice of magnetic materials and their grade is managed by particular magnetic applications which balance extrinsic magnetic properties as coercitivity (H_c) and remanence (B_r). Traditionally, high coercitivity and elevated working temperatures of ternary Nd-Fe-B magnets are achieved by the substitution of Nd metal for heavy rare-earth as Dy and Tb in Dy, Tb – containing high-coercitivity permanent magnets. The addition of heavy rare-earth metals increases magnetocrystalline anisotropy of $(Nd_{1-x}RE_x)_2Fe_{14}B$ phase proportionally to the addition of heavy rare-earth metal. The correlation between magnetic anisotropy field and coercitivity is described by $H_c=\alpha H_A-N_{eff}M_s$, where M_s is saturation magnetization, α is a structural coefficient depending on grain boundaries of main $(Nd,Dy)_2Fe_{14}B$ magnetic phase, and N_{eff} is effective demagnetization factor describing the inhomogeneity in microstructure (the amount and grain size of the secondary phases and main phase, etc.) [4, 5]. However, antiferromagnetic interaction between heavy rare-earth atoms (Dy or Tb) and Fe atoms of Dy doped $(Nd,Dy)_2Fe_{14}B$ phase leads to the decrease of saturation magnetization M_s and remanence B_r.

An alternative approach to the heavy-rare earth alloying is based on the microstructure enhancement providing α close to 1 with a simultaneous decrease of Neff. This concept requires a strong compromise between H_c and M_r due to the presence of secondary phases. The secondary Nd-rich phase plays a key role in liquid phase sintering, pinning site forming and weakening of the exchange interaction between the grains of the main phase [4]. It is well known that single-crystalline $Nd_2Fe_{14}B$ magnets have low Hc because domain wall motion during the demagnetization occurs at a very low demagnetization field [5]. Demagnetization can take place at a negative magnetic field due to the high demagnetization factor of a single-crystal sample. High coercitivity is possible only in the presence of pinning centres that inhibit the movement of the domain wall or suppress reverse magnetization domains in the magnetically isolated highly dispersed grains. Magnetic domains are inevitable on the surface of Nd-Fe-B magnets due to surface imperfections [4, 5]. Therefore, the pinning centres must exist along the grain boundaries, so that the propagation of the magnetic domain is suppressed starting from the grain surface itself to the nearest grains, which have large scattering fields [5, 6].

Large pinning forces occur if there is a critical change in the constant of magnetocrystalline anisotropy in a narrow range, ie $H_c \approx t(A_m/A_s-K_s/K_m)$, where A_s, A_m are exchange and K_s, K_m magnetocrystalline anisotropy constants of secondary and main phase accordingly, t – the second phase thickness.

Since all sintered permanent magnets are multiphase polycrystals, the centres of pinning are grain boundaries or intergranular phases. Recent studies of high coercitivity heavy rare-earth free Nd-Fe-B magnets (H_{cj}=2 T) have suggested that H_c of anisotropic polycrystal magnets depends on grain size regardless of the nature of the magnetism of the boundary between the

grains of the main phase (Fig. 1). The grain boundary of the main phase can be both paramagnetic in the exchange-decoupled or ferromagnetic in the exchange-coupled structures [6].

If there is no exchange interaction between ferromagnetic grains due to the nonmagnetic grain boundary or intergranular phase, demagnetization occurs by the formation of domains with reverse magnetization on a single grain. This requires a certain amount of secondary non-magnetic phase, so it is necessary to control the balance between H_c and M_r.

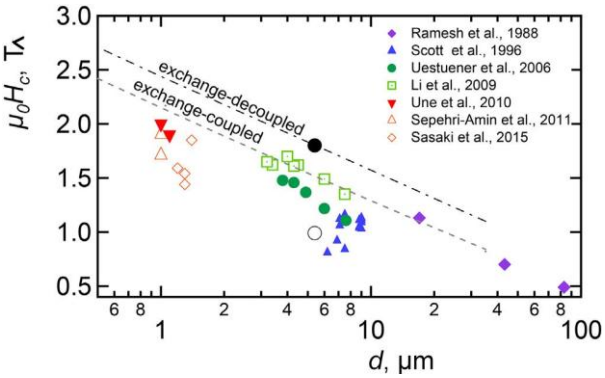

Fig. 1. Coercivity vs. grain size for sintered Nd-Fe-B magnets [4]

Until recently, the main mechanism of coercitivity in sintered Nd-Fe-B magnets was considered to be the formation of reverse magnetization domains on defects, such as grain boundaries or disordered grains. The main thesis of this mechanism was the complete isolation of the grains of the main magnetic phase by the layer of the non-ferromagnetic (paramagnetic) secondary phase. The smooth magnetization curve was evidence of the absence of pinning centres. However, if the distance between the pinning centres is larger than the grain size, which contains many domains, ie its size is a priori larger than the size of one magnetic domain, then the original magnetization curve will be equally smooth without the influence of pinning centres.

Recent scientific papers on the commercial sintered magnets, using three-dimensional atomic analysis (3DAP), have shown that the structure and chemical composition of a thin intergranular layer about 3 nm thick, which turned out to be a ferromagnetic $Fe_{65}Nd_{34}Cu_1$ (at. %) phase. Magnetic properties of the intergranular phase were studied by spin-polarised scanning electron microscopy and X-ray magnetic circular dichroism [7]. However, electron holography measurements showed slightly higher Ms (about 1 T) of the intergranular phase [8].

Providing that grains of the main magnetic phase in the sintered Nd-Fe-B magnets are magnetically isolated, coercitivity is attributed to the reverse magnetization domains on the surface defects as grain boundaries or triple points. Triple points possess the highest demagnetization field. Thus, coercitivity corresponds to the Stoner-Wolfart ratio, and the largest demagnetization field will be if the axes of the $Nd_2Fe_{14}B$ phase grains coincide with the direction of the external magnetic field, ie in the sample with high crystal-graphic texture (001), which was confirmed by micromagnetic data calculation [4, 9, 10]. However, experimental data revealed a decrease in H_c when the texture coefficient $\beta = M_r/M_s$ approaching 1, where 0.5 – isotropic, 1 – textured samples.

This indicates the insensitivity of Hc to the degree of ordering (texturing). Although in magnets with an average level of magnetic properties (Hc up to 800 kA/m, and grain size 5 μm) the magnetization curve does not show the behaviour inherent in the pinning model, grain boundary pinning appeared in high coercitivity magnets with a direct exchange between magnetic grains, across the ferromagnetic boundary. It is typical for heavy rare-earth free magnets with reduced grain size [11] or fine microstructure (melt-spinning) [12]. A similar shape of the magnetization curve is observed in magnets obtained by die-upsetting of melt-spun ribbons, in which the grain size coincides with the size of a single domain [12].

The conventional production process of Nd-Fe-B magnets consists of sintering (T=950…1150°C) and two-stage heat treatment (T=950…1150°C and T=550…600°C). The second stage of low-temperature annealing usually increases the H_c by a quarter. Advanced microstructure techniques allow studying the boundary layers between the grains of the main $Nd_2Fe_{14}B$ phase, to determine their atomic composition and propose a mechanism that explains increased magnetic hardness.

Hence, heavy rare-earth free Nd-Fe-B magnets possess several types of grain boundaries that have a strong influence on the H_c mechanism. Whereas the demagnetization in exchange-decupled magnets occurs individually in each grain because of the thin non-ferromagnetic boundary layer, avalanche-like advancement of domain walls takes place in exchange-coupled magnets. Despite the advantage of high coercitivity in exchange-decoupled magnets, the squareness of their demagnetization curves may partially deteriorate [6]. One of the ways to improve the squareness of demagnetization curves is to reduce the grain size and increase the texture of the main $Nd_2Fe_{14}B$ phase.

One way to improve the magnetic texture and coercitivity of Nd-Fe-B magnets is to use PLP (pressless process) proposed by M. Sagawa [13, 14]. The greatest advantage over the conventional powder metallurgy method lies in the container sintering without pressing the powders [13, 14]. By eliminating pressing procedure, PLP resulted in a higher degree of powder alignment and provided the automation of the rather arduous production stages – placing the powder to the container, green part magnetizing and further sintering. Moreover, the geometry of the PLP magnet is very close to the final shape that will enable minimal polishing or its complete absence. Additionally, increased sealing of the equipment reduces the oxygen adsorption and allows to use fine powders (< 1 μm). The fine powder of about 1 μm size yield a single-domain grain size of $Nd_2Fe_{14}B$ phase with increased coercitivity in sintered heavy rare-earth free magnets. The key aspect of PLP technology is the use of highly dispersed micron-size powders that are very prone to oxidation. This requires special protecting conditions and advanced approaches to avoid critical degradation.

In this study, we used improved powder alignment and almost net-shape production of the magnets via PLP

and we present a new method that gives optimum grain size and distribution of the powders.

2. EXPERIMENTAL PROCEDURE

To produce magnets via PLP, $Nd_{33}Fe_{65.9}B_{1.1}$ (wt. %) cast alloy was ball-milled in the ethyl acetate as protecting medium. Two containers were freely filled with ball-milled powder. The containers were made of stainless steel and ceramic. The densification of the powders was performed by vertical positioning of the container on the vibrating table. The ceramic container was upturning several times during vibrating to guaranty smooth densification. Then container was magnetized in the field of 5 T. The magnetization was carried out two times in one direction and once in the opposite one to get a high magnetic texture. The powders in the containers were sintered for 55 min at T=1050°C and then subjected to heat-treatment for 30 min at T=830°C.

Magnetic measurements were performed by fluxmeter after sintering and heat treatment. The composition and structure of PLP magnets were analyzed through SEM using a JSM-7001F microscope.

3. STRUCTURE AND MAGNETIC PROPERTIES OF HIGH-PERFORMANCE ND-FE-B MAGNETS PRODUCED BY PLP METHOD

Given that modern industry stands high tolerance requirements to the sintered permanent magnets, PLP can bring the benefit of net-shape manufacturing just under careful adherence to technological regimes at all stages of production.

It seems very interesting to apply the PLP method to the production of magnets of various shapes. For example, it can be the sintering of long blanks with their subsequent cutting. The present paper presents a combination of wet-milled powders and their sintering in the container.

Table shows the weight loss, shrinkage coefficient and magnetic parameters of sintered PLP magnets. The weight loss revealed the lack of any obvious correlation and was mostly attributed to the ethyl acetate vaporisation during the compacting stage.

N sample	m_{in}, g	$m_{sint.}$, g	m_{in}-m_{sint}, g	ρ_{app}, g/cm^3	K_{II}	$K_{\perp}$	Magnetic flux after sintering., a.u.	Magnetic flux after heat-treatment., a.u.
1510_3-2	8.5	8.2	0.3	2.4	1.37	1.4	5.2	-
2510_12-2	30.3	28.7	1.6	2.4	1.43	1.43	5	-
1210_3-2	8.49	7.9	0.59	2.43	1.46	1.49	5.3	5.44
2909_25-3	22.6	21.1	1.5	2.47	1.49	1.39	5.38	4.32
1010_3-2	8.7	8.4	0.3	2.48	1.44	1.45	5.24	5.12
2809_25-1	22.69	21.7	0.99	2.48	1.42	1.46	4.87	4.7
1010_25-1	23.5	21.1	2.4	2.57	1.47	1.43	5.2	5.07
2510_3-2	9.1	8.4	0.7	2.64	1.46	1.4	5.1	-
910_3-_3	9.64	9	0.64	2.75	1.41	1.4	5.44	4.8
1910_3-2	10.3	10.2	0.3	3	1.43	1.35	4.3	-
2010_3-2	10.6	9.9	0.7	3	1.46	1.34	5.15	4.9
2210_21-2d	65.7	62.8	2.9	3	1.3	1.31/1.5	4.69	4.69
1210_25-1	28.8	26.2	2.6	3	1.27	1.36	5.13	4.3
1510_25-3	28.8	27.6	1.2	3	1.48	1.34	5	-
2910_3-2	10.8	10.2	0.6	3.13	1.39	1.3	5	-

The as-sintered magnet samples are shown in Figs. 2 and 3. It can be seen that the direction of the magnetic field during compaction strongly affected the shrinkage behaviour. This shrinkage behaviour is influenced by different sintering coefficients of the samples depending on the crystallographic direction. Whereas the shrinkage coefficient of the c-axis is about 1.41, it is close to 1.39 for the normal direction. Moreover, the apparent density affected the ratio between the sintering coefficients in the direction of the anisotropy and normal to it (Fig. 4). The increase in the apparent density has resulted in better densification of the sample in the axial direction. The densification coefficient of the diametrically magnetized sample is about 1.1-1.14. It can be visually seen as an ellipse cross-section (see Fig. 3).

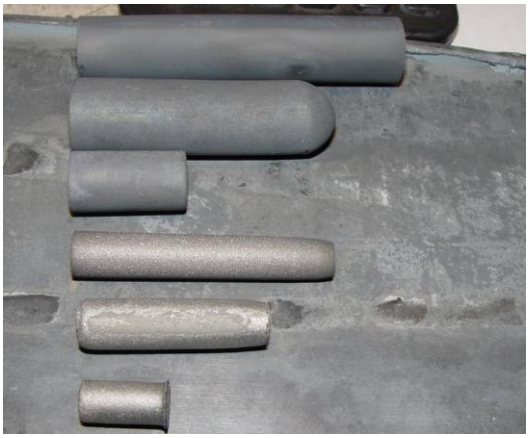

Fig. 2. General view of long-length PLP magnets

ISSN 1562-6016. ВАНТ. 2021. №6(136)

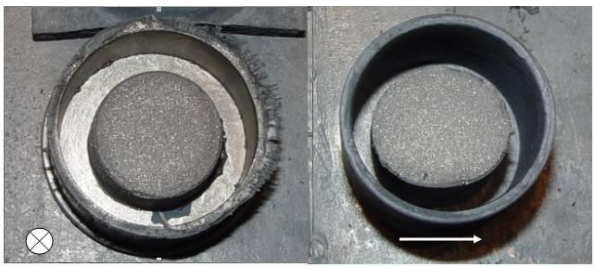

Fig. 3. General view of PLP magnets – axial and diametral magnetization

All samples that were sintered in the container and undergone three times pulsed magnetization in the axial direction have a very low divergence in diameter along the entire length of the sample. This allows making a small allowance for grinding and thus significantly save the material at the stage of machining.

The density of sintered PLP samples is about 7.35…7.4 g/cm^3, which is practically the same as for the conventional powder metallurgy approach – magnetizing and pressing powders in the moulds. However, it was revealed that the magnetic properties of finals samples correlated well with apparent density.

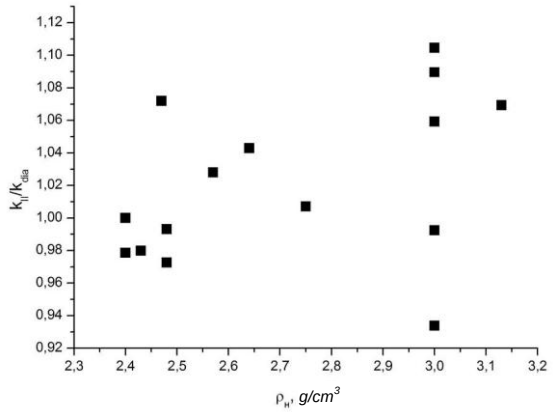

Fig. 4. Correlation between shrinkage coefficient ratio ($K_{II}/K^{\perp}$) and apparent density

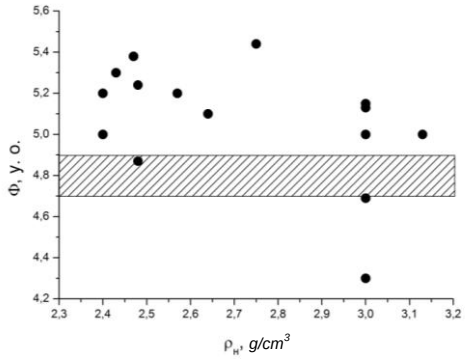

Fig. 5. The magnetic flux of PLP magnets versus apparent density (shad line – typical magnetic flux of conventional powder metallurgy technology)

Fig. 5 illustrates the dependence of magnetic flux on apparent density. It can be seen that the magnetic flux of PLP magnets is noticeably higher than in magnets produced by conventional powder metallurgy way. Some magnet flux decrease with increased apparent density is the result of slight misalignment due to higher densification. Anisotropic densification during the sintering stage is related to the difference in thermal expansion coefficients of the $Nd_2Fe_{14}B$ phase. According to Popov [15], magnetoelastic coupling below Curie temperature leads to the non-uniform contacting forces between powder particles depending on texture direction and anisotropic grain growth. The latter takes place both under crystallization and recrystallization.

It appears from this work that PLP magnets, especially with high aspect ratio l/d, needs ad-hoc optimization of the PLP. A slight drop of magnetic flux after heat treatment is typical for Nd-Fe-B based magnets due to recrystallisation of the main phase and a small decrease of Hc.

This work suggests that the vertical or horizontal placement of the container in the vacuum furnace affected the shrinkage coefficient along with magnetic texture. Whereas the shrinkage coefficient is about 1.41 for horizontal sintering, it reaches 1.49 for vertical one because of gravity.

4. MAGNETIC MATERIALS UNDER IRRADIATION

A major challenge of magnetic materials used in technological electron accelerators is the high resistance to the demagnetization under irradiation.

The present work focuses on the study magnetic properties of $Nd_{33}Fe_{65.9}B_{1.1}$ and Sm_2Co_{17} based alloys under electron irradiation and bremsstrahlung in the energy range matching main technological accelerators of NSC KIPT [16 - 18].

Direct electron beam treatment of Nd-Fe-B magnets with the energy of 10 MeV resulted in a considerable change of magnetic flux and its distribution. The degree of magnetic flux degradation was correlated to the irradiation dose. Re-magnetization of Nd-Fe-B magnets after irradiation returns their magnetic properties to the initial state – both magnetic flux and its distribution.

Prior work on the irradiation of SmCo magnets under the same energy of 10 MeV shows that the absorbed dose of 16 Grad and bremsstrahlung kept the magnetic performance of SmCo magnets almost the same. Even a ten-fold increase of absorbed dose did not lead to any significant change in magnetic properties.

When the Nd-Fe-B magnets are irradiated with electrons at an energy of 23 MeV, a loss of magnetic properties is also observed [17]. However, bremsstrahlung generated by electron beam does not change the magnetic flux of Nd-Fe-B samples. The residual activation at these energies of the SmCo alloy samples is so great that it makes it impossible to use this material for the manufacture of magnetic devices and their operation under real working conditions.

5. MAGNETIC SYSTEMS FOR TECHNOLOGICAL ACCELERATORS

Two dipole magnets were developed and manufactured at NSC KIPT to work on beams of electron accelerators [18, 19].

SmCo magnets were used for the upgraded 10 MeV electron accelerator. The SmCo based magnetic system is applied to the measurement and control of beam energy. Fig. 6 shows the general view of the dipole magnet.

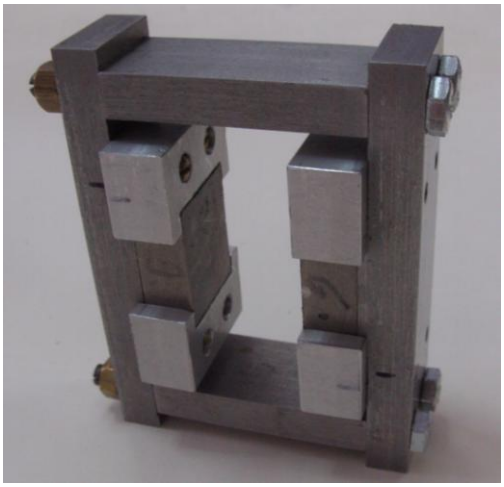

Fig. 6. General view of SmCo magnetic system of 10 MeV electron accelerator

The external dimensions of the magnetic circuit are 90×73×27 mm. It is made of steel 3 soft magnetic steel. The accuracy and positioning of components are 5 μm. The upper bar of the dipole magnet is removable. This makes it easy to mount and remove the dipole magnetic system on the accelerator output flange during the measurement or energy adjustment procedure of the accelerator.

The Peak magnetic field of the dipole magnet is 0.311 T. The effective length along the central beam trajectory is 33.53 mm.

The upgrade of the linear electron accelerator "EPOS" is aimed at manufacturing a new channel with a rotation of the 23 MeV electron beam by 90 degrees. To eliminate the effect of the electron beam on the Nd-Fe-B magnet, a special design of the magnetic system was chosen. As can be seen in Fig. 7, key point is to remove the block of magnets from the beam as much as possible and to exclude the direct effect of electrons on the magnet material.

Fig. 7. General view of Nd-Fe-B magnetic system of 23 MeV electron accelerator

The dimension of the Nd-Fe-B based magnetic system of 23 MeV electron accelerator are 233×170×435 mm.

The magnetic field in the gap is formed by a magnetic circuit and magnetic poles made of steel 3.

The highest magnetic field in the range of 0.516…0.493 T can be achieved in the gap of 25 mm at T=23…40°C. The effective length of the magnetic system calculated on the trajectory of a particle with the energy of 23 MeV in the field of 0.516…0.493 T is (242±1.1) mm. An accelerator thermostat system can be used to stabilize the magnetic performance of the magnetic system. To do this, a system of copper cooling tubes is installed in the body of the magnetic circuit.

In many cases, accelerators need to transport the electron beam over long distances. Doublets and triplets of quadrupole lenses are used to form the beam. As shown in K. Halbach [20], multipole magnetic devices can be designed using permanent magnets. These ideas were later implemented on many accelerators [1 - 3]. At the same time, as we have already noted, the design of quadrupole lenses was chosen to take into account the peculiarities of operation on a specific accelerator. To work on beam transportation paths on technological accelerators of NSC KIPT, it is assumed to develop quadrupoles with a gradient of 6…7 T/m, designed to work with beams up to an energy of 60 MeV.

SUMMARY

In summary, it is shown that PLP technology can be effectively used in the production of high-performance permanent magnets for further application in technological accelerators. PLP permanent magnets became a critical component of dipole and quadrupole magnetic systems of the electron accelerators. We have studied the magnetic performance of Nd-Fe-B and SmCo magnets under irradiation, which allows to make an optimal choice of material and design the devices taking into account the parameters of the accelerator.

REFERENCES

1. B.J.A. Shepherd. Permanent magnets for accelerators // *11th Int. Particle Acc. Conf. IPAC2020, Caen, France.* 2020, p. 6-10.
2. C. Benabderrahmane. Review of Permanent Magnet Technology for Accelerators // *8th International Particle Accelerator Conference, Copenhagen, Denmark*. 2017, May 14-19.
3. F. Marteau et al. Variable high gradient permanent magnet quadrupole (QUAPEVA) // *Applied Physics Letters*. 2017, v. 111, p. 253503-1-5.
4. K. Hono, H. Sepehri-Amin. Strategy for high-coercivity Nd-Fe-B magnets // *Scripta Materialia*. 2012, v. 67, issue 6, p. 530-535.
5. Y. Matsuura, N. RintaroIshii, M. Natsumeda, J. Hoshijima, F. Kuniyoshi. Temperature properties of the alignment dependence of coercive force decrease ratio and the angular dependence of coercive force in Nd-Fe-B sintered magnets // *J. Magn. Magn. Mater*. 2016, v. 398, p. 246.
6. K. Hono, H. Sepehri-Amin. Reprint of Prospect for HRE-free high coercivity Nd-Fe-B permanent magnets // *Scripta Materialia*. 2018, v. 154, p. 277-283.
7. T. Kohashi, K. Motai, T. Nishiuchi, S. Hirosawa. Magnetism in grain-boundary phase of a NdFeB sintered magnet studied by spin-polarized scanning electron microscopy // *Appl. Phys. Lett.* 2014, v. 104, p. 232408.

8. T. Nakamura, A. Yasui, Y. Kotani, T. Fukagawa, T. Nishiuchi, H. Iwai, T. Akiya, T. Ohkubo, Y. Gohda, K. Hono, S. Hirosawa. Direct observation of ferromagnetism in grain boundary phase of Nd-Fe-B sintered magnet using soft x-ray magnetic circular dichroism // *Appl. Phys. Lett.* 2014, v. 105, p. 202404.
9. J. Fujisaki et al. Micromagnetic Simulations of Magnetization Reversal in Misaligned Multigrain Magnets With Various Grain Boundary Properties Using Large-Scale Parallel Computing // *IEEE Transactions on Magnetics.* 2014, v. 50, № 11, p. 1-4, Nov. Art no. 7100704.
10. Yutaka Matsuura, Jun Hoshijima, Rintaro Ishii. Relation between $Nd_2Fe_{14}B$ grain alignment and coercive force decrease ratio in NdFeB sintered magnets // *Journal of Magnetism and Magnetic Materials*. 2013, v. 336, p. 88-92.
11. H. Sepehri-Amin, Y. Une, T. Ohkubo, K. Hono, M. Sagawa. Microstructure of fine-grained Nd-Fe-B sintered magnets with high coercivity // *Scripta Materialia*. 2011, v. 65, p. 396-399.
12. J. Liu, H. Sepehri-Amin, T. Ohkubo, K. Hioki, A. Hattori, T. Schrefl, K. Hono. Grain size dependence of coercivity of hot-deformed Nd-Fe-B anisotropic magnets // *Acta Mater.* 2015, v. 82, p. 336-343.
13. M. Sagawa, Y. Une. A new process for producing Nd-Fe-B sintered magnets with small grain size // *Proc. 20th Int. Workshop on Rare Earth Permanent Magnets and Their Applications.* Knossos, Crete, 2008, p. 103-105.
14. M. Sagawa. Development and prospect of the Nd-Fe-B sintered magnets // *Proc. of 21st Int. Workshop on REPM and their Applications*. Bled, Slovenia, 2010, p. 183-410.
15. A.G. Popov, A.V. Shitov, E.G. Gerasimov, D.Yu. Vasilenko, M.Yu. Govorkov. Obtaining sintered Nd-Fe-B magnets without a powder pressing process // Physics of Metals and Metalscience. 2012, № 113(4), p. 352-362 (in Russian).
16. M.I. Ayzatsky et al. The NSC KIPT electron linacs – R&D // *Problems of Atomic Science and Technology. Series "Nuclear Physics Investigations"*. 2003, № 2, p. 19-25.
17. V.A. Bovda et al. Radiation induced demagnetization of permanent magnets under 10 MeV electron beam // *Problems of Atomic Science and Technology. Series "Nuclear Physics Investigations"*. 2016, № 6, p. 13-16.
18. V.A. Bovda et al. Nd-Fe-B magnets under electron irradiation with the energy of 23 MeV // *Problems of Atomic Science and Technology. Series "Nuclear Physics Investigations"*. 2020, № 3, p. 23-27.
19. V.A. Bovda et al. Two dipole magnetic systems for technological electron accelerator // *Problems of Atomic Science and Technology. Series "Nuclear Physics Investigations"*, 2019, № 6, p. 9-12.
20. K. Halbach. Design of permanent multipole magnets with oriented rare earth cobalt material // *Nucl. Instrum. Methods.* 1980, v. 169, p. 1-10.

Article received 04.10.2021

ПРИМЕНЕНИЕ РЕДКОЗЕМЕЛЬНЫХ МАГНИТОВ ДЛЯ СОЗДАНИЯ МАГНИТНЫХ СИСТЕМ ТЕХНОЛОГИЧЕСКИХ УСКОРИТЕЛЕЙ ЭЛЕКТРОНОВ

В.А. Бовда, А.М. Бовда, И.С. Гук, В.Н. Лященко, А.О. Мыцыков, Л.В. Онищенко

Высокоэнергетичные редкоземельные постоянные магниты становятся главными компонентами современных электронных ускорителей. Описана технология изготовления магнитов с высокими магнитными характеристиками на основе сплавов редкоземельных элементов методами порошковой металлургии. Исследованы изменения магнитных свойств образцов магнитов при воздействии на них электронного пучка и тормозного излучения электронов с энергиями 10 и 23 МэВ. Разработаны дипольные магниты с постоянным полем для технологических электронных ускорителей ННЦ ХФТИ.

ЗАСТОСУВАННЯ РІДКОЗЕМЕЛЬНИХ МАГНІТІВ ДЛЯ СТВОРЕННЯ МАГНІТНИХ СИСТЕМ ТЕХНОЛОГІЧНИХ ПРИСКОРЮВАЧІВ ЕЛЕКТРОНІВ

В.О. Бовда, О.М. Бовда, І.С. Гук, В.Н. Лященко, А.О. Мициков, Л.В. Оніщенко

Високоенергетичні рідкоземельні постійні магніти стають головними компонентами сучасних електронних прискорювачів. Описано технологію виготовлення магнітів з високими магнітними характеристиками на основі сплавів рідкоземельних елементів методами порошкової металургії. Досліджено зміни магнітних властивостей зразків магнітів при впливі на них електронного пучка і гальмового випромінювання електронів з енергіями 10 і 23 МеВ. Розроблено дипольні магніти з постійним полем для технологічних електронних прискорювачів ННЦ ХФТИ.